AAS 14-267

DESIGN OF END-TO-END TROJAN ASTEROID RENDEZVOUS TOURS INCORPORATING POTENTIAL SCIENTIFIC VALUE

Jeffrey Stuart*, Kathleen Howell†, and Roby Wilson‡

The Sun-Jupiter Trojan asteroids are celestial bodies of great scientific interest as well as potential natural assets offering mineral resources for long-term human exploration of the solar system. Previous investigations have addressed the automated design of tours within the asteroid swarm and the transition of prospective tours to higher-fidelity, end-to-end trajectories. The current development incorporates the route-finding Ant Colony Optimization (ACO) algorithm into the automated tour generation procedure. Furthermore, the potential scientific merit of the target asteroids is incorporated such that encounters with higher value asteroids are preferentially incorporated during sequence creation.

INTRODUCTION

Near Earth Objects (NEOs) are currently under consideration for manned sample return missions,[1] while a recent NASA feasibility assessment concludes that a mission to the Trojan asteroids can be accomplished at a projected cost of less than $900M in fiscal year 2015 dollars.[2] Tour concepts within asteroid swarms allow for a broad sampling of interesting target bodies either for scientific investigation or as potential resources to support deep-space human missions. However, the multitude of asteroids within the swarms necessitates the use of automated design algorithms if a large number of potential mission options are to be surveyed. Previously, a process to automatically and rapidly generate sample tours within the Sun-Jupiter L_4 Trojan asteroid swarm with a minimum of human interaction has been developed.[3] This scheme also enables the automated transition of tours of interest into fully optimized, end-to-end trajectories using a variety of electrical power sources.[4,5] This investigation extends the automated algorithm to use ant colony optimization, a heuristic search algorithm, while simultaneously incorporating a relative 'scientific importance' ranking into tour construction and analysis. The proposed tour creation strategy is not specific to the problem of asteroid missions and, therefore, the low-thrust tour design concept is readily applied to a diverse range of prospective mission scenarios.

High-efficiency, low-thrust propulsion systems are particularly attractive for missions to the Sun-Jupiter equilateral equilibrium points because of the relatively stable natural gravitational dynamics in these regions. Propellant-optimal, low-thrust trajectories, realized by constant specific impluse

*Ph.D. Candidate, Purdue University, School of Aeronautics and Astronautics, 701 W. Stadium Ave., West Lafayette, IN, 47906, (765) 620-4342, jrstuart@purdue.edu.

†Hsu Lo Distinguished Professor of Aeronautics and Astronautics, Purdue University, School of Aeronautics and Astronautics, 701 W. Stadium Ave., West Lafayette, IN, 47906, (765) 494-5786, howell@purdue.edu.

‡Supervisor, Inner Planet Missions Analysis Group, Mission Design and Navigation Section, Jet Propulsion Laboratory, California Institute of Technology, 4800 Oak Grove Dr., Pasadena, CA 91109, (818) 393-5301, roby.s.wilson@jpl.nasa.gov.

vehicle systems in nonlinear dynamical regimes, typically require coasting arcs and the careful balancing of engine capability with transfer time. Therefore, a variable specific impulse (VSI) engine that varies the optimal thrust magnitude is selected to simplify the construction of rendezvous solutions.[6] As a consequence, no coasting arcs are required for rendezvous and the initial generation of optimal trajectories is less restrictive in terms of thrust duration. Examples of VSI engines include the Variable Specific Impulse Magnetoplasma Rocket (VASIMR) currently under development by the Ad Astra Rocket Company[7] and the Electron and Ion Cyclotron Resonance (EICR) Plasma Propulsion Systems at Kyushu University in Japan.[8] Though a VSI engine model is employed to generate preliminary trajectories, specific tours of interest can be transitioned to models incorporating higher fidelity current- and near-term engine models. For example, high specific impulse portions of the VSI thrust arcs may be replaced by coast arcs for corresponding constant specific impulse (CSI) systems and spacecraft and mission parameters may be adjusted to better reflect current propulsion capabilities.

While event timing and propellant requirements are critical components in mission design and analysis, other driving factors contribute to the creation and selection of prospective trajectories. For asteroid tour scenarios, an important consideration is the relative scientific value attached to particular asteroids or specified combinations of asteroids, that is, the relative value in terms of scientific data or resource discovery for specific asteroid sequences. Thus, tour design schemes that incorporate a relative priority or importance metric, either within sequence generation or as part of data post-processing, can be a valuable tool in satisfying scientific or economic mission objectives as well as technical requirements. This investigation presents various schemes to incorporate this priority consideration both as part of post-creation sequence analysis as well as an integrated component of tour creation.

Even in the most simplified form, tour design is an NP-hard problem, meaning that the solution space grows exponentially with a linear growth in the number of potential targets. Therefore, once targets have been selected and transition options, with the associated costs, have been computed (if pre-computation of these links is even feasible), a computationally efficient search method must still be implemented. While strict tree enumeration is a practical scheme for very small scale problems, this solution method quickly becomes intractable for even moderately-sized problems. Thus, many graph search methods, such as Dijkstra's algorithm[9] and branch-and-bound tree searches,[10] have been developed over the years. One heuristic algorithm based upon the foraging behavior of ants, ant colony optimization (ACO),[11] has gained much interest as a solution scheme for a wide variety of applications, from the classic Traveling Salesman Problem (TSP) to routing of information in data networks to the organization of jobs within a factory.[12] While ACO has a history of successful implementation in discrete system formulations, the algorithm also has the potential to be adapted to scenarios with continuous trade-spaces, such as astrodynamics. Thus, a modified form of ACO suitable for smooth solution spaces is applied to the generation of asteroid tours as well as compared to the operation of enumerated searches.

POTENTIAL SCIENTIFIC MERIT OF TARGET ASTEROIDS

The Trojan asteroids as a whole offer great potential for valuable scientific insight; however, specific target asteroids may possess uncommon or even unique characteristics that warrant higher priority in mission planning scenarios. The Trojan asteroids reside in two clusters around the Sun-Jupiter L_4 and L_5 libration points, the more numerous "Greek" and smaller "Trojan" camps, respectively. Twelve target asteroids from the larger L_4 swarm are selected for this preliminary inves-

tigation, where the asteroids all reside in generally low inclination orbits with respect to the solar system ecliptic. However, these objects still possess a range of physical characteristics that serve to distinguish them and allow for a relative ranking of potential scientific merit. Indeed, two target asteroids, 624 Hektor and 3548 Eurybates, are included specifically because they offer the possibility of higher than average scientific returns. Table 1 lists the target asteroids along with their osculating orbital elements on October 3, 2021 and the relative priority ranking used in this investigation. The following sections detail the scientific considerations that aid in distinguishing higher priority targets among the selected asteroids.

Table 1. Asteroids selected as bodies of potential scientific interest in the L_4 Trojan asteroid swarm. Osculating orbital elements at epoch 3 Oct. 2021.

Name	a**, AU**	e	i**, deg**	Ω**, deg**	ω**, deg**	θ^***, deg**	**Priority,** w
624 Hektor	5.25	0.023	18.16	342.9	187.7	236.8	2
659 Nestor	5.14	0.116	4.53	350.8	342.3	69.4	1
1143 Odysseus	5.21	0.090	3.14	221.3	239.3	277.0	1
1869 Philoctetes	5.16	0.064	3.98	43.9	325.2	8.9	0.5
3548 Eurybates	5.19	0.088	8.06	43.6	27.0	342.7	2
4057 Demophon	5.22	0.118	2.88	24.3	61.6	288.2	0.5
4138 Kalchas	5.15	0.043	2.10	208.1	162.8	36.0	1
5012 Eurymedon	5.24	0.084	5.00	34.8	333.6	25.6	0.5
5652 Amphimachus	5.19	0.074	1.90	281.8	102.7	11.7	0.5
7152 Euneus	5.13	0.061	3.71	113.1	307.7	332.0	0.5
8241 Agrius	5.15	0.044	4.34	22.7	264.6	132.1	0.5
8317 Eurysaces	5.30	0.047	0.94	208.2	113.2	92.9	0.5

Asteroid Spectral Types

The Sun-Jupiter Trojan asteroid swarm is composed of two distinct spectral groupings, D-type asteroids that are a dark burgundy hue (the so-called "redder" group) as well as C- and P-type asteroids that possess a more blue-grey color (the "less-red" set).[13,14] These observations from the NASA Infrared Telescope Facility and the WISE telescope indicate that the L_4 Trojan asteroid swarm is composed of primordial bodies that have a composition that may be distinct from the brighter red main belt asteroids as well as the icy Kuiper belt objects. In fact, these asteroids are among the oldest extant bodies in the solar system and may be the only remaining samples from this region of the early accretion disk. Any prospective spacecraft tour of the Trojan swarm that encounters at least one object from each spectral group, therefore, offers a much greater potential for scientific return than a comparable tour that encounters objects of only one, or of unknown, spectral type. Of the twelve target asteroids in this preliminary investigation, two (624 Hektor and 1143 Odysseus) are D-type, redder objects and three (659 Nestor, 3548 Eurybates, and 4138 Kalchas) are in the less-red group. Thus, these asteroids have been assigned a slightly higher priority value of 1

(or higher, in the special cases of 624 Hektor and 3548 Eurybates), above the 0.5 scientific metric assigned to asteroids of unknown spectral type.

624 Hektor - Contact Binary

In addition to its classification in terms of spectral type, the redder asteroid 624 Hektor garners interest because it is the only known example of a contact binary in the "Greek" camp in the vicinity of the L_4 Sun-Jupiter libration point.[15,16] This highly oblong object is also larger than most other Trojan asteroids, equivalent in size to a 225-km diameter spheroid. Furthermore, observations from the Keck telescope have confirmed the presence of a 15-km diameter moonlet in orbit around the main body.[17] The roughly 1,200-km altitude, 2.98-day orbit of this moonlet suggests an estimated bulk density of 1.8-3.5 g/cm^3 for the main body of asteroid 624 Hektor. Proximity operations at 624 Hektor can offer valuable insight into the nature of binary systems as well as an evaluation of the bulk density estimates. Thus, a rendezvous encounter with Hektor is given an elevated priority of 2 in this preliminary investigation.

3548 Eurybates - Collision Family

Similarly to 624 Hektor, less-red 3548 Eurybates is prioritized as a high-value target because it is believed to be the main remnant of an asteroid-asteroid collision.[18] Even though this collision is estimated to have occured 1-4 Gyr in the past, at least 150 asteroids are still grouped by physical and orbital properties such as spectral type and semi-major axis in the vicinity of 3548 Eurybates, indicating a significant collision event. Thus, a spacecraft encounter with Eurybates can offer key insights into such asteroid-asteroid collisions. Furthermore, the approach and departure for the main collision body can also afford fly-by opportunities with collision ejecta, further increasing the scientific value of a rendezvous with 3548 Eurybates. Though these fly-by opportunities are not explicitly modeled in this investigation, the increased fly-by potential and opportunity to examine a large collision fragment does warrant an higher priority level of 2 for encounters with 3548 Eurybates.

TOUR GENERATION OVERVIEW

While previous papers describe the base asteroid tour generation process in more detail,[4,5,3] a brief overview of the scheme is presented for clarity. In general, tours are constructed by sequencing variable specific impulse (VSI) low-thrust arcs drawn from pre-computed, independently generated families of locally optimal rendezvous solutions. The individual arcs are computed using a constant-power model for the electric engine wherein the thruster continually operates at the maximum allowable power $P_{\max}$. The tour sequencing is analyzed via an enumerated tree search where propellant costs and timing are approximated for the full tour using data from the independent thrust arcs. While this largely automated method reliably produces advantageous tours of the Trojan asteroids, the computational cost of the enumerated search scheme scales exponentially with the inclusion of additional target asteroids and the restriction to single pre-selected thrust intervals does not fully exploit the design space represented by the families of low-thrust solutions. Thus, while the enumerated tree search procedure is used to generate tours incorporating the scientific merit of the asteroids, it also serves as a baseline comparison for the ant colony optimization algorithm.

Creation of Asteroid-Asteroid Rendezvous Families

For even a relatively small number of asteroids, manually determining and generating all possible optimal rendezvous arcs is a laborious process. For example, for any given pair of asteroids, there are several epochs over the specified 40-year mission window (Oct. 3, 2021 to Oct. 3, 2061) that define a locally optimal departure state for a rendezvous arc. So, when all possible asteroid pairs are considered, hundreds of locally-optimal rendezvous arcs are available for any given thrust duration (TD). Therefore, an automated scheme that detects conditions amenable to locally optimal transfers and, subsequently, computes the corresponding point solutions is critical for rapid trajectory design.

Conditions likely to yield optimal transfers include low distance and low relative velocities between asteroids. One efficient strategy to detect these transfer conditions searches epochs for those that correspond to the minimum relative distance between an asteroid pair. Thus, solutions to the local optimization problem

$$\min d_a(t_0) = \|\boldsymbol{r}_T(t_0) - \boldsymbol{r}_I(t_0)\| \tag{1}$$

supply the initial guesses for the parameter t_0 in the rendezvous problem. Thus, the problem involves only one free parameter, and a grid search readily produces all the solutions over the 40-year window of opportunity. Once the set of initial parameters t_0 is determined, a hybrid optimization scheme incorporating indirect optimal thrust control laws with the direct local optimization of a mass objective function is applied to generate thrust arcs connecting the paths of the asteroids.

The hybrid optimization process yields a single rendezvous segment connecting two asteroids and resulting in a trajectory arc with minimum propellant consumption for a specified thrust duration. The initial and terminal states along these arcs correspond to approximate asteroid positions and velocities from the CR3BP dynamical model such that the spacecraft is delivered from the vicinity of one asteroid to that of another. However, once a point solution is generated for a single specified thrust duration, TD, a simple continuation scheme is applied that produces trajectory arcs over a large range of thrusting times. The continuation process updates the value of TD and uses the previously computed solution as the initial guess for the subsequent 2PBVP. The complete set of thrust arcs that is determined via the continuation scheme, termed a "family", represents a set of options for a single pre-determined asteroid-to-asteroid link within a design space relating engine operation time and propellant consumption for a spacecraft transfer. For this analysis, families of transfer arcs between any asteroid pair with thrust durations between $TD = 0.7$ and a nominal maximum $TD = 2.0$ in non-dimensional time units, incremented in steps of 0.02 non-dimensional time units, or 483 to 1379 days in 14 day steps, are produced. Some families do not cover the full range of thrust durations since the iteration process is terminated once the epoch expands to the limits of the window, i.e., Oct. 3, 2021 to Oct. 3, 2061. Note that for every thrust arc segment within these families, the initial spacecraft mass is assumed to be $m_0 = m_r = 500$ kg, or $m_0 = 1$ non-dimensional unit. (Of course, this initial mass may be adjusted in the tour construction process.) Once the independent solutions comprising the families of rendezvous arcs are computed, the initial conditions are stored for future use; this set of stored initial conditions is termed a "library".

Rendezvous Sequence Construction

To generate a potential tour sequence, an automated process extracts independent families of arcs from the library of solutions, selects individual rendezvous legs from within these families, and combines them into a series of thrust arcs between the asteroids and coast segments in the vicinity of the objects. This selection and joining of independent thrust arcs is performed via an enumerated

tree search wherein all potential new targets are exhaustively searched. Figure 1 illustrates the operation of the tree search method. Note that for NP-hard problems enumerated tree searches quickly become computationally expensive and can be replaced with other search methods such as branch-and-bound.

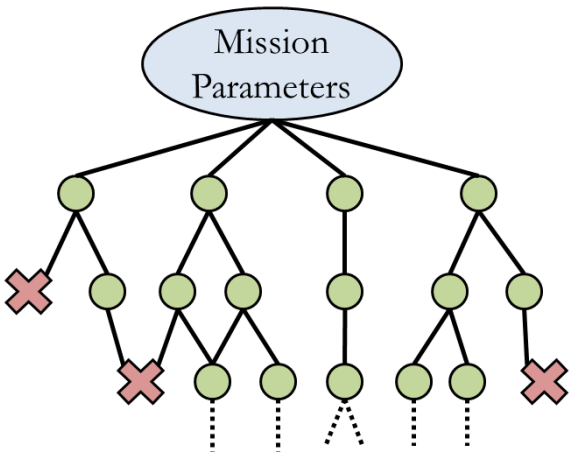

Figure 1. Schema of the enumerated tree search algorithm. Note that, in general, intermediate target asteroids (green circles) or terminal asteroids (red X's) can appear on multiple paths.

Since there are many possible thrust arcs across any given family, and the tree search procedure extracts only one solution arc per family, a trade-off is available between thrust duration TD, departure epoch τ_0, and arrival mass m_f. In general, m_f increases with TD while τ_0 decreases; however, it is observed that the quantity $(TD+\tau_0)$ usually increases with larger values of TD. For this investigation, the tour sequence algorithm allows the user to select one of three possible thrust duration options over all families in a potential sequence: (i) maximum TD and, therefore, maximum m_f and arrival epoch with minimum τ_0; (ii) minimum TD, with the reverse result; (iii) median TD, with median values of arrival mass and departure and arrival epochs. Once specific thrust arcs are selected, approximations are employed to estimate the performance metrics associated with a particular tour. For example, propellant consumption during each interval of engine operation must be incorporated into an equivalent cost corresponding to any potential tour scenario comprised of several rendezvous arc segments. Accordingly, for a rendezvous sequence built from n thrust intervals, the approximate consumption of propellant mass, m_{cons}, is computed via

$$m_{consumed} = m_0\left(1 - \prod_{i=1}^{n} \frac{m_i}{m_0}\right) \tag{2}$$

where m_i is the arrival mass in kilograms at the end of the i^{th} independently generated thrust arc.* For feasible options, this easy to compute approximation can always be evaluated against a more rigorous model, such as an end-to-end optimization.

Since the families representing asteroid-to-asteroid transfer arcs are independently created, the selected rendezvous sequences must be evaluated to ensure they are physically realizable and satisfy mission constraints. Frequently, the two most common constraints in mission design are propellant

*For the case of impulsive maneuvers, an equivalent total trajectory cost is $\Delta v_{tot} = \sum_{i=1}^{p} \Delta v_i$ where Δv_{tot} is the total impulsive Δv and Δv_i is the equivalent value for one maneuver.

mass and mission duration, i.e., a finite amount of mass is available and a limited opportunity usually exists for a timeline. Therefore, a maximum amount of propellant is available for activities within the swarm m_p and a maximum mission duration, TOF, is specified in the automated tour design scheme. Thus, for a tour to be feasible, the estimated propellant consumption, m_{cons}, must be less than m_p and the final rendezvous must occur before $t_a + TOF$ where t_a is the epoch corresponding to swarm arrival. Additionally, since the goal is survey options for missions to the Trojan asteroids, a further constraint is imposed, that is, the spacecraft cannot re-visit an asteroid after departure. Ultimately, the arc selection procedure is summarized in Table 2. The result

Table 2. Arc selection procedure for tour generation via enumerated tree search.

Step	Description
1	Select specific desired asteroid arrival epoch and thrust duration options as well as specify asteroid swarm propellant mass m_p and mission timeline TOF.
2	For each asteroid of interest, perform Steps 3-8.
3	Retrieve from library all thrust arc families departing from current asteroid.
4	Remove families that return to previously visited asteroids.
5	For given TD option, eliminate all families with departure epochs prior to the current feasible departure epoch or beyond the arrival epoch $t_a + TOF$.
6	Estimate spacecraft mass at end of all thrust arcs and remove families where $m_{cons} > m_p$.
7	For the remaining families, update tour information to include data from new arcs.
8	Repeat Steps 3-7 until the exploration of all possible tours is complete.

of the sequence construction procedure is a set of potential tours with estimated propellant mass consumption values less than m_p and with total time within the swarm that is less than (TOF) years. Performance metrics include propellant consumed, swarm tour duration, coast time in the vicinity of the asteroids, as well as the number and merit of asteroid encounters; specific sequences of interest are then selected for further analysis.

Results Incorporating Scientific Merit

Inclusion of the potential scientific merit of the individual target asteroids is included as a post-processing step in the tour generation scheme from previous studies.[3,5,4] Recall that this sequencing procedure uses an enumerated tree search over a limited sub-set of the rendezvous arcs from the full library of pre-computed solutions, i.e., only one asteroid-asteroid leg of pre-specified thrust duration TD is evaluated per family. Potential rendezvous legs are added to tour sequences so long as they do not violate either the propellant budget of the spacecraft or limits on the mission window. The spacecraft and mission parameters used in this investigation, unless otherwise noted, are presented in Table 3. As previous investigations demonstrate,[4] these values can be readily altered and are used here strictly for demonstration purposes. Once a set of potential tours is constructed, the individual merits of the encountered asteroids are summed for each tour, resulting in a prospective mission priority ranking. Particular tours of interest can then be transitioned to higher fidelity models if desired.

Table 3. Spacecraft and tour parameter values.

Quantity	Value
Swarm arrival spacecraft mass (m_r), kg	500
Propellant available in swarm (m_p), kg	150
Tour window in swarm (TOF), yrs	10.5
Reference engine power ($P_{\max}$), kW	1.0
Selected arc duration from family	Median TD

Tours originating from all twelve asteroids are generated over a 25-year window of initial epochs, from 2021 to 2046, that is all tours that are 10.5 years in duration, arrive no sooner than 2021, and end operations no later than 2057 are discovered. Figure 2 synthesizes the results into a glyph plot representing the relative performance of each initial target asteroid. As noted in the figure, the objects are compared according to the number of tours available, the number of encounters per tour, and the relative merit ranking of potential tours. Two initial asteroids, namely 624 Hektor and 1143 Odysseus, provide good all-around performance relative to other objects when selected as the initial target, while three others (5652 Amphimachus, 7152 Euneus, and 8317 Eurysaces) provide good performance in all categories except the number of high-priority tours (that is, cumulative scientific merit of 4 or larger). What is intriguing about the latter three asteroids is that they individually possess low priority, but they seem to provide ample opportunity to transfer to other, more meritritious, asteroids within the swarm. On the other extreme, 3548 Eurybates and 8241 Agrius seem to offer the least overall options, though the high scientific priority of 3548 Eurybates does ensure that it provides a relatively large number of high merit tours.

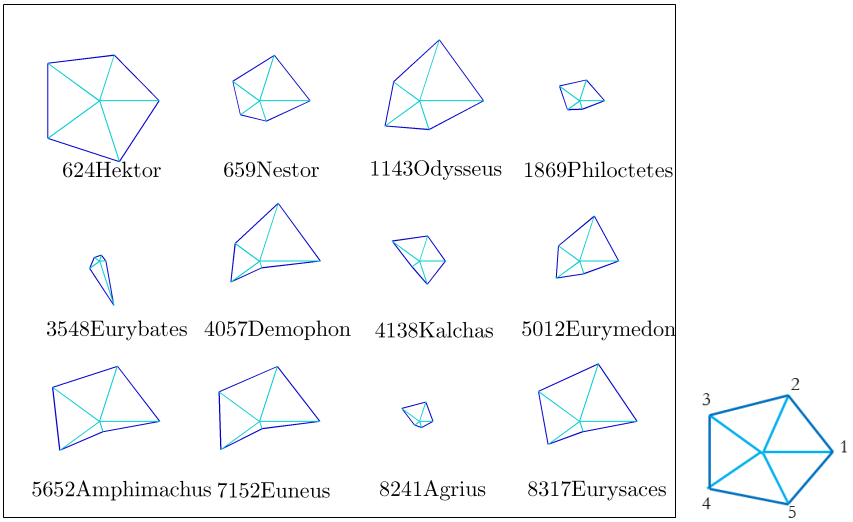

Figure 2. Aggregate searches for all twelve target asteroids. For comparison of relative lengths, the spokes are: 1) average number of tours per year, 2) average number of tours encountering 3 asteroids, 3) average number of tours encountering 4 or more asteroids, 4) average merit of all tours, 5) average number of tours with priority 4 or higher.

Examining tours orginating from 3548 Eurybates in more detail provides further insight not only into advantages of selecting this asteroid as the initial encounter but also the peformance of the other potential targets. Averages of the number of asteroids visited per tour and the average merit of the tours over the 25-year swarm arrival window are computed and displayed in Fig. 3. Both averages have a cyclical pattern with a peak-to-peak period of approximately 11 years; intuitively, higher merit opportunities correspond to years when the average number of encounters per tour is approximately 3 or higher. Though not shown in this investigation, these trends in the number of encounters and merits of the tours are exhibited by tours originating at other initial target asteroids. Note that even though there are some initial epochs where only two asteroid tours are available, other swarm arrival years offer ample tours with 3 or even 4 asteroid encounters. Recalling the relative performance of 3548 Eurybates from Fig. 2, the inference can be made that most tours within the swarm and with the parameters specified in Table 3 offer encounters with at least 3 target objects.

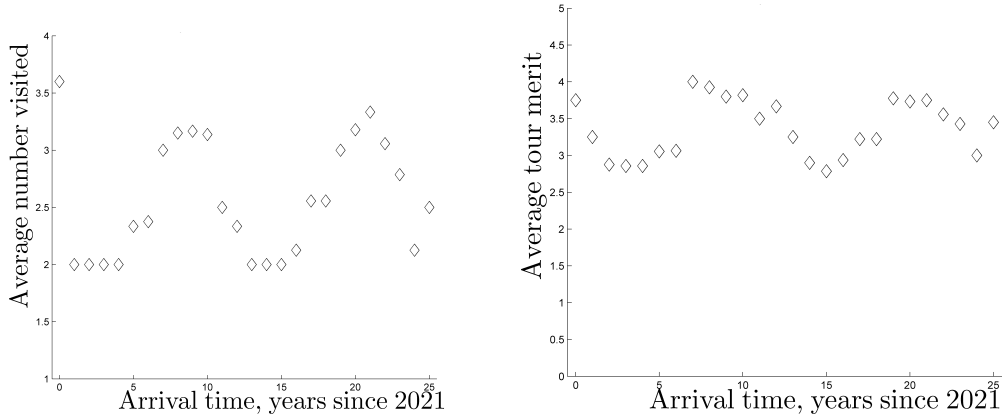

a. Average number of encounters per tour. b. Average tour priority.

Figure 3. Yearly search averages for tours originating at asteroid 3548 Eurybates.

One more step in the selection of specific tours of interest is to examine the potential tours for one swarm arrival epoch; as a demonstration, the asteroid 624 Hektor is selected as the initial target and an arrival in the year 2026 is chosen. The tour generation scheme produces a set of 15 viable tours, 14 of which encounter 3 asteroids. Propellant, ΔV, and proximity operation time estimates for the tours are displayed in Fig. 4, where the tours have been ranked in descending order by total scientific merit. Note that propellant consumed and tour ΔV are directly related while the distribution of proximity operation times near the encountered asteroids shows a few patterns consistent with multiple potential tours using identical transfer arcs. For example, the three highest ranked tours all follow the same rendezvous leg from 624 Hektor to 3548 Eurybates and thus have the same duration spent in the vicinity of the initial target asteroid. However, each tour has a distinct tertiary target and therefore present options for duration near 3548 Eurybates and total tour propellant cost. The third ranked tour is selected for further investigation because it offers long intervals at both of the highest value target asteroids, 624 Hektor and 3548 Eurybates, and a final short duration in the vicinity of 8241 Agrius. For this tour, the spacecraft path through physical space and the thrust profiles of the VSI engine are presented in Fig. 5. Note the large out-of-plane motion of the tour, consistent with the relatively high inclinations of the target asteroids. On the other hand, the 624 Hektor to 3548 Eurybates rendezvous arc has a thrust profile that is roughly consistent in magnitude and is thus readily transferable to a constant specific impulse mission architecture while the second rendezvous

arc could be replaced with two thrust intervals with an intermediary coast interval. As shown in previous studies,[5,4] transitioning this potential tour to a higher fidelity model is a straight-forward, automated process.

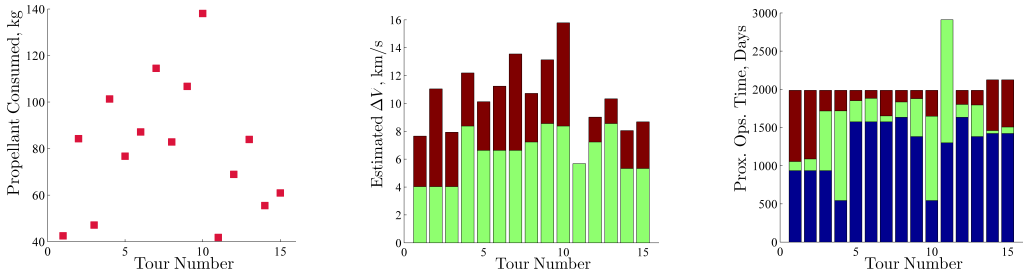

a. Propellant consumed, per tour. b. Tour ΔV, by leg. c. Prox. Ops. time, by encounter.

Figure 4. Performance of tours originating from 624 Hektor with swarm arrival in 2026.

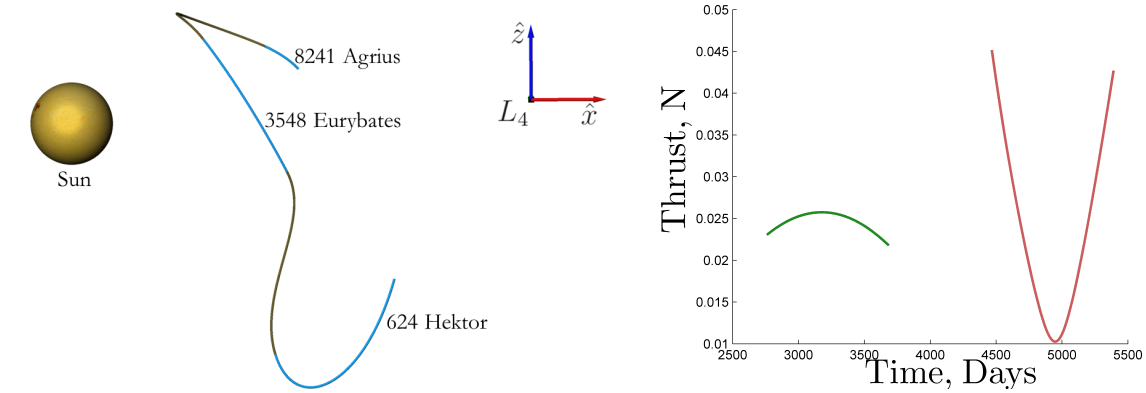

a. Trajectory, rotating frame, view from ecliptic plane. Blue coast arcs near asteroids, gold thrust arcs.

b. Thrust profiles. Time is days since 3 October 2021.

Figure 5. Tour originating at 624 Hektor and encountering 3548 Eurybates and 8241 Agrius.

ANT COLONY OPTIMIZATION

Ant colony optimization is a robust and adaptable hueristic search algorithm with many NP-hard applications beyond astrodynamics and mission planning. However, several modifications must be made to the typical implementation of ACO to fully exploit the search spaces and the trade-offs available in trajectory design. The details in traditional ACO are highlighted below and expanded capabilities are introduced for the design of asteroid rendezvous tours.

Standard ACO

Standard ant colony optimization (SACO) is a stochastic route-finding algorithm patterned after the foraging behavior of ant colonies wherein ants alternately explore for food and follow pheromone trails to known food sources. Once a source of food is discovered, the ants instinctively locate a route that is near-optimal in travel distance to the food while retaining the ability to adapt to changing environments and opportunities. The process relies on the continued laying and dissipation of pheromone trails such that favorable trails are reinforced while other routes decay as

they are not used. This process is inherently robust while ensuring close to optimal performance as well as allowing for a variety of static and dynamic applications.

Typical SACO applications assume a discrete set of N targets, or nodes, with single, bi-directional links between them, such that an "ant" traveling from location A to location B can equally easily travel in the opposite direction for the same cost. As illustrated in Fig. 6, these networks are usually sparse, that is, not every pair of nodes is connected. In most applications, the goal is to traverse the network from one node to another or to create a circuit of all nodes, both for the least cost. Furthermore, many SACO applications simplify the model to one cost, for example, travel time between cities in the classic Traveling Salesman Problem (TSP). To construct the most efficient route, multiple generations of ants are released wherein each individual ant travels from node to node by following these behavioral procedures at each encountered node:

1. *Exploration*: With some probability γ, travel to a randomly selected new node, where the parameter γ decreases from 1 to some steady-state value $0 < \gamma_{ss} < 1$ over succeeding generations; else,

2. *Following*: Stochasitcally select an unvisited node with the probability

$$P_{i,j} = \frac{\tau_{i,j} B_{i,j}^{\beta}}{\sum \tau_{i,j} B_{i,j}^{\beta}} \tag{3}$$

   where $P_{i,j}$ is the probability for traveling from the i^{th} node to the j^{th} node, $\tau_{i,j}$ is the pheromone level on the link, $B_{i,j}$ is the quality of the connection, and β is a weighting parameter.

3. When the ant reaches the desired target destination, terminate search.

The number of ants used, i.e., N_a is an adjustable parameter in the algorithm. After each succeeding generation of ants, the pheromone levels along each individual link are updated via

$$\tau_{i,j} = (1 - \rho)\tau_{i,j} + Q_{i,j} \tag{4}$$

with decay rate ρ and pheromone update $Q_{i,j}$. Note that this pheromone increase, $Q_{i,j}$, corresponding to a given link is often either zero (if only the best routes and, therefore, the best links, are reinforced) or some function that is dependent on the performance metric associated with tours that include the particular leg in question. A common pheromone update procedure involves an increase of the pheromone on each link of the best tour by the summed quality of each link on said tour, that is

$$Q = \sum_{j=2, i=j-1}^{N_e} B_{i.j} \tag{5}$$

where $Q = Q_{i,j}$ for each (i, j) link on the best tour and N_e is the total number of nodes traversed. Under this update model, the best tour acquires the highest Q value. A variation on this update strategy is an assignment of this same pheromone increase across all tours. After a pre-determined number of generations, this procedure is terminated and the best tour is returned. Due to the stochastic nature of the algorithm and the recognized tendency of ACO algorithms to quickly "lock" onto potential solutions, several runs are typically completed and the best route from among the runs is

returned as the solution. For ACO algorithms as a whole, local information is supplied by the link quality, $B_{i,j}$, while global "goodness" information is preserved in the pheromone concentrations, $\tau_{i,j}$. Thus, in most SACO applications, the number of generations, number of ants, γ, β, ρ, and selection criteria for pheromone updates are all adjustable parameters.

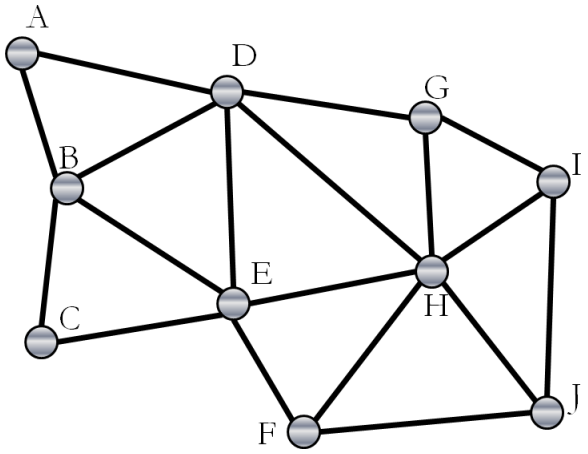

Figure 6. Schema of sample network on which ant colony optimization can be applied. Links between objects can be traveled in both directions.

ACO with Parallel Pheromone Distribution

While SACO can, in practice, be applied to mission planning scenarios, several considerations point to a novel ACO solution approach, one that may in fact be a more true mimicry of actual ant foraging behavior than is typical of SACO. One chief difference between spacecraft trajectory applications of ACO and more traditonal ACO scenarios is that astrodynamics problems typically involve an infinite number of potential connections between celestial objects of interest rather than a single link. Furthermore, many SACO applications either intrinsically possess easy-to-compute link costs or scenarios are readily abstracted to a simplified model whereas mission analysis and design must maintain a higher level of model fidelity in order to ensure viable resulting trajectories. Thus, rather than a sparse network with a relatively low number of analytically modeled links between nodes, astrodynamics applications typically present a very dense grid of connections, each possessing a unique but infinite trade space that generally must be constructed numerically. While large portions of these trade spaces can be eliminated due to physical, logistical, or other practical considerations, there still remains an infinite possible number of solutions due to the continuous nature of the underlying dynamics. Thus, a discretization of the search space is required, though this may still result in very large search spaces. For example, in the current investigation, roughly 36,000 individual thrust arcs are constructed computationally between asteroid pairs for a set of 12 objects over a 40-year window. However, these rendezvous arcs are grouped into 551 families characterized by the close approach epochs between asteroid pairs and offering a trade-off between thrust duration and propellant consumption.

The highly correlated nature of the asteroid-asteroid rendezvous legs within distinct families naturally leads to the concept of ACO with parallel pheromone distribution (ACO-PPD), that is, ACO wherein successful tours spread pheromone to nearby links as well. Thus, if an individual arc from a family is part of a successful tour, then some amount of pheromone is applied to solutions in the family with similar thrust duration values ("parallel" solutions), as illustrated in Fig. 7. Accordingly,

when the ants are following pheromone trails, the potential to explore nearby solutions also exists which could offer improved performance over the previously traveled sequence. The distributed pheromone can be spread to any number of arcs within the family, although, in practice, a balance is struck between increasing the number of potential solutions to explore and maintaining a low computational overhead (i.e., if pheromone is spread to all possible arcs, the compuational cost for one ant approaches that of an enumerated tree search algorithm). The distribution over the nearby arcs can also be modeled from one of several profiles: for the current investigation, both uniform and Gaussian distributions of pheromone are considered. When normal distributions are employed, the standard deviation is assumed to be

$$\sigma = \sqrt{N_{ps}} \tag{6}$$

where N_{ps} is the one-sided number of arcs over which the pheromone is spread (i.e., if $N_{ps} = 5$, pheromone is placed on 11 members of the family, i.e., the traveled leg plus 5 solutions with larger TD values and 5 with lower durations). While the current implementation generates tours using pre-computed low-thrust arcs between asteroids, ACO-PPD can be readily adapted to support a diverse range of mission planning architectures.

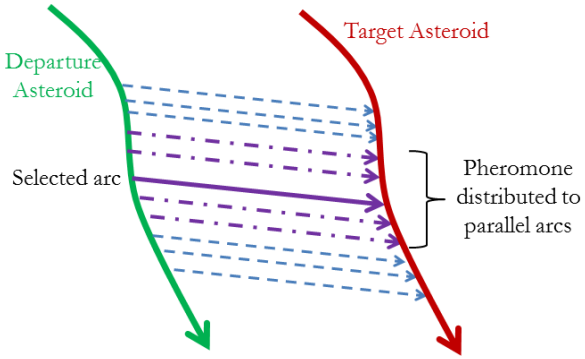

Figure 7. Diagram of asteroid-asteroid family with traveled arc and pheromone distributed to nearby thrust legs.

Generation of Asteroid Tours

Though pheromone distribution supplies a powerful framework for extending ACO to astrodynmics applications, several implementation details remain to fully incorporate ACO-PPD to the generation of asteroid tours. Notably, link costs are often more complex for spacecraft trajectories than most SACO applications. Additionally, SACO usually assumes that all nodes must be transited for the least cost or that the optimal route from one specific node to another is desired (note that the latter case is analogous to the determination of the optimal trajectory from Earth to another planet, say Jupiter or Saturn). However, for the construction of asteroid tours, it is not feasible to visit all potential targets with one trajectory and selecting specific target asteroids *a priori* may unduly restrict preliminary explorations of the design space. In fact, the concept of an "optimal" spacecraft tour is heavily dependent on the relative weighting assigned to propellant and operations costs, the desired number of objects, relative scientific value of various targets, and many other considerations. Thus, this investigation expands SACO and ACO-PPD concepts to favor options beyond optimal route-finding, e.g., the best selection of potential targets within the context of limited resources. This implementation of an ACO-PPD strategy may, in fact, produce a better model of ant scavenging behavior than previous SACO applications.

When not actively following pheromones, ants explore by randomly selecting a previously unvisited target asteroid and tracking the first feasible family (characterized by the rendezvous leg of median thrust duration TD value) that links the current asteroid to the target asteroid. If no families linking these two specific asteroids include a feasible median TD arc, the destination asteroid is discarded and a new target is randomly selected. If all asteroids are excluded by this procedure, then the ant terminates its tour. Ant exploration behavior is triggered under the following circumstances:

- at the current node, *exploration* is selected based upon the exploration probability γ; or,
- if *following* is identified, then either no pheromone exists on arcs departing the current asteroid or none of the pheromone trails satisfy time or propellant constraints.

Using these conditions, the ants are guaranteed to continue encountering new asteroids until the limits on total time-of-flight or maximum propellant capacity are reached. For the current implementation of ACO-PPD, the exploration probability in the k^{th} generation is defined to be

$$\gamma = \gamma_{ss} + (1 - \gamma_{ss}) e^{-\frac{k-1}{\ln N_g}} \tag{7}$$

where γ_{ss} is the lowest desired exploration probability and N_g is the number of generations of ants. This definition of exploration probability ensures a smooth exponential decay from a probability of 1 in the first generation to the base probability, γ_{ss}. The natural logarithm term provides a consistent decay of exploration likelihood regardless of the number of generations selected.

A crucial aspect of ACO is the definition of the link quality metric, i.e., $B_{i,j}$, that conveys local information to traveling ants and aids in the determination of the travel probability represented in Eq. (3). For asteroid tour applications, one potential metric is

$$B_{i.j} = \frac{w_j^W p_{i,j}^M}{\Delta t_{i,j}^L} \tag{8}$$

where w_j is the target importance, $p_{i,j}$ is the propulsive cost to travel from object i to the j^{th} asteroid, $\Delta t_{i,j}$ is the time to travel from one object to the next, and W, M, and L are weighting parameters. For Trojan asteroid tours, the target importance w_j is set equal to the scientific priorities in Table 1 and the propulsive cost is defined to be $p_{i,j} = m_{f:i,j}$, that is, the arrival mass along the independently computed thrust arc. The time metric is defined as $\Delta t_{i,j} = t_{f:j} - t_{f:i}$, that is, the difference in arrival epochs between the next asteroid and current asteroid; note that this value includes the loiter time at the current asteroid as well as the transit time between the current object and the next encounter. Thus, Eq. (8) is reformulated as

$$B_{i.j} = \frac{w_j^W m_{f:i,j}^M}{\Delta t_{i,j}^L} \tag{9}$$

where all required information is available either from the pre-computed thrust arc families or the pre-specified asteroid priority.

While SACO implementations often specify that the overall quality of a solution is a simple summation of the link costs across the sequence, other methods of defining tour quality are available. Recall that for the current investigation, the individual link quality metric $B_{i.j}$ includes the relative priorities concerning time, propellant, and target, all of which are locally important. However, the

tour quality value Q that informs the update to pheromone levels can represent any combination of local and global information across the tour sequence and, hence, affords another level of control over the performance of the algorithm. Therefore, several different formulations of 'tour quality', summarized as follows, are examined:

- *Summed link quality*: This tour quality metric is consistent with many SACO implementations by summing the individual link quality corresponding to each tour via

$$Q = w_1^W + \sum_{j=2, i=j-1}^{N_e} B_{i,j} \tag{10}$$

  where N_e is the total number of asteroid encounters. Only the merit of the first target is included as Earth-to-asteroid legs are not considered in this ACO investigation.

- *Number of encounters*: Tours are ranked solely upon the number of asteroids encountered, without regard to propellant cost or asteroid priority such that

$$Q = N_e. \tag{11}$$

- *Summed object merit*: Quality of tours is determined by summing the importance of the encountered asteroids by

$$Q = \sum_{j=1}^{N_e} w_j \tag{12}$$

  where a fewer number of higher priority targets could elevate its ranking over a tour to a larger number of less important objects.

- *Combined importance and loiter time*: The importance of the asteroids is multiplied by the duration of proximity operations at the object and then summed as

$$Q = \sum_{j=1}^{N_e} w_j LT_j \tag{13}$$

  where LT_j is essentially the loiter time, i.e. the interval spanning the arrival at the j^{th} object to departure from the same asteroid. Thus, tours that include longer durations at higher priority targets are favored. However, a maximum useful loiter time $LT_{\max}$ can be instituted such that any proximity duration above this threshold is not incorporated into Eq. (13).

Each of these tour quality definitions, aside from the summed link quality, allows for the tour quality to be developed independently of the local behavior of the ants. A related factor is the number of ants N_{sa} that lay pheromone trails. Any implementation where the number of pheromone laying ants is less than the total number of ants, i.e., $N_{sa} < N_a$, necessitates a ranking of the ants by their respective tour qualities Q. For ACO-PPD implemenations, a larger value for N_{sa} allows more pheromone spread and, hence, a broader survey of the design space while a lower number focuses on improvement in the few best routes.

Similar to the recognized tendency for ACO algorithms to rapidly "lock" onto known routes, ACO-PPD may concentrate ants along only a few highly favorable encounter sequences within

the first few ant generations. While this behavior may allow a more thorough exploration of the continuous trade spaces associated with particular asteroid progressions, it may also neglect other advantageous target sequences. Thus, a selection criteria to favor unique series over rendezvous chains with identical orders of encounter, but possibly a different set of individual arcs, has also been included. With this option, unique successions of asteroids are placed ahead of all but the highest quality examples of repeated sequences; for example, if three of the top asteroid series include a repeated encounter progression but differing individual legs, then only the best performing example is retained and the remaining two are placed behind all the potential tours with unique asteroid orders.

Finally, seeding the initial distribution of the ants for each generation supplies another level of input into the ACO implementation process. Two methods are employed in this investigation, namely i) randomly distributing ants to seed each generation, or ii) for each ant, based upon current exploration probability γ, either place it at a random starting location or stochastically locate the ant at a starting node based upon pheromone concentrations departing the nodes. In the latter case, the probability at being placed at the i^{th} asteroid is given by

$$P_i = \frac{\sum_{j=1}^{N_p} \tau_{i.j}}{\sum_{i=1}^{N_{ast}} \sum_{j=1}^{N_{p:i}} \tau_{i.j}} \tag{14}$$

where N_{ast} is the total number of asteroids and $N_{p:i}$ is the total number of links with pheromone departing the i_{th} asteroid. Consistent with previous options, random assignment of the initial object favors exploration for good sequences while ant placement based upon pheromone concentration benefits the more thorough exploitation of a fewer number of sequences. Note, however, that even though an initial target is not selected *a priori*, the current implementation of ACO-PPD does require a pre-specified swarm arrival epoch.

Comparison to Enumerated Tree Search

While this investigation does not include a rigorous benchmark comparison between ant colony optimization and other graph search methods, some predictions about ACO-PPD performance relative to enumerated tree searches can be made. Recall, as an example, the set of 15 distinct asteroid sequences originating from 624 Hektor for the swarm arrival epoch of 2026; this set of tours, averaging nearly three asteroid encounters, is a fairly conservative representation of the average performance, in both number of tours discovered and number of encounters per tour, exhibited by the enumerated tree search scheme. Assuming that each pre-computed family represented in the asteroid tours contains 66 members, fully assessing each potential combination of thrust arcs within a tour requires 4356 operations. Thus, fully characterizing the trade space associated, that is, all possible sets of thrust arcs associated with the employed rendezvous families within all tours, with one initial target asteroid requires approximately 65,340 computations and, therefore, examining all 12 potential targets necessitates on the order of 784,000 operations for just one swarm arrival epoch. These numbers, of course, discount the possibility that, even for identical asteroid sequences, different combinations of individual asteroid-asteroid legs may engender or preclude further potential encounters (i.e., one set of arcs from a three asteroid sequence may enable the spacecraft to visit a fourth target, while a different combination consumes too much propellant for the spacecraft to reach any further objects). Furthermore, the number of operations to fully enumerate the tour trade space grows exponentially with each additional asteroid added to the search.

Ant colony optimization, even with distributed pheromones, offers a much more managable growth in computational cost. Assuming, as before, an average of 3 asteroids per tour, with an average of 20 members per family with pheromone, each ant requires on the order of 400 operations to create a tour. If 25 ants are used per generation (resulting in approximately 10,000 computations per generation), over 78 generations of the ACO-PPD algorithm would be required to match the computational cost of the 12-asteroid enumerated tree search performed at the same epoch (recall that the current implementation of ACO-PPD necessitates the *a priori* selection of an arrival epoch) and that assesses all possible members of each family of rendezvous solutions. This, of course, does not consider that at each asteroid several departure rendezvous families, with associated pheromones, may be assessed before the selection of the next target. On the other hand, this figure assumes that every ant always follows pheromone trails and neglects the significant computational cost savings when exploration behavior is selected (as it will be for a relatively significant proportion of any ACO run). Furthermore, the computational cost of the ACO-PPD algorithm is relatively fixed, regardless of the number of target asteroids. Thus, ACO-PPD offers significant advantage when larger numbers of asteroids are included in the tour creation process.

ACO-PPD: Sample Results

The ACO-PPD algorithm is applied to the construction of tours within the L_4 Trojan asteroid swarm; several runs are made, each with a distinct set of parameters so that the effect of the various options on the performance of the algorithm may be assessed. A set of parameters common to all the runs is defined in Table 4 while additional parameters that differ by ACO-PPD run are presented in Table 5. As the goal is tours that explore the L_4 asteroid swarm, ants are specified to not return to asteroids they have already encountered. Furthermore, Case 7, which uses the combined importance and loiter time tour quality metric, has a specified $LT_{\max}$ of 517 days, or approximately 1.4 years, such that loiter times longer than this maximum value are capped at 517 days when constructing the tours.

Table 4. Spacecraft, tour, and ACO-PPD parameter values, common to all runs.

Quantity	Value
Swarm arrival spacecraft mass (m_r), kg	500
Propellant available in swarm (m_p), kg	150
Tour window in swarm (TOF), yrs	10.5
Reference engine power ($P_{\max}$), kW	1.0
Swarm arrival year	2026
Number of generations (N_g)	50
Link quality weight in link probability (β)	1
Pheromone spread size (N_{ps})	5
Number of ants to lay pheromone (N_{sa})	5
Base exploration probability (γ_{ss})	0.1
Selected arc duration from family (exploration)	Median TD

Table 5. ACO-PPD parameter values that differ among runs.

Quantity	Case Values							
	Base	**1**	**2**	**3**	**4**	**5**	**6**	**7**
Number of ants (N_a)	25	20						
Pheromone distribution	Uniform	Gauss						
Link quality weights	$M = 1$ $L = 1$ $W = 0$					$M = 0$ $L = 1$ $W = 0$	$M = 1$ $L = 1$ $W = 1$	
Tour quality metric (Q)	Link Quality		Number	Merit Sum				Priority Loiter
Favor unique	Yes				No			
Ant placement	Random				Pher.			

*Empty cells indicate value is identical to base set of parameters.

The characteristics of the highest ranked tour from each run are summarized in Table 6, where the different ACO-PPD parameters engender varying amounts of divergence from the performance of the base run. Note that the row for "Merit $\times$ Prox. Ops. Time" is computed via the link quality definition in Eq. (13); thus, this metric provides a sense of the proportion of time spent at high potential scientific return objects. The base set of parameters, as well as Cases 1 and 2, results in the creation of a tour that encounters 5 asteriods, namely 1143 Odysseus, 4138 Kalchas, 8317 Eurysaces, 659 Nestor, and 5652 Amphimachus, within 10.5 years; note that this tour was not generated by an equivalent enumerated tree search using only single links from the rendezvous families. Thus, ACO-PPD has the potential to bring forth tours not available to schemes that do not fully access the potential trade spaces offered by rendezvous opportunities. Furthermore, the 5-asteroid sequence did not emerge from the run for Case 4, which did not favor unique encounter orders and placed ants at targets with higher pheromone concentrations, showing that certain parameter options can counter, to some extent, the reported tendency for ACO to "lock" into solutions. On the other hand, parameter sets that incorporate the target priority typically result in sequences with fewer encounters but generally higher potential for scientific return. Notabley, Cases 3, 6, and 7 generate target orders that were discovered via the simplified tree search scheme (specifically, 624 Hektor, 3548 Eurybates, and 659 Nestor for Cases 3 and 6 contrasted with 624 Hektor, 3548 Eurybates, and 8241 Agrius for Case 7), however the ACO-PPD runs do result in the selection of individual thrust arcs that tend to increase the tour quality metric above that of tours from the enumerated search. While certain sets of ACO-PPD parameters do result in similar qualitative results, each case offers a distinctly different quantitative result for the highest ranked tour (e.g., Cases Base, 1 and 2 produce the same sequence but provide different options for proximity duration and propellant consumption). The notable exceptions to this behavior are Cases 3 and 6, which generate identical tours, albeit with slightly different run times. For all sets of ACO-PPD parameters, the largest effect on the run time are the number of ants per generation (as evidenced by Case 1 that only employs 20 ants compared to all other cases that use 25 ants) and whether the parameters will favor tours with more

or fewer encounters (generally, cases that produce tours with a larger number of asteroids in the sequence will require more computations). Though not an exhaustive examination of all possible combinations of ACO-PPD, spacecraft, and mission parameters, these cases do highlight the power and versatility of ant colony optimization when applied to astrodynamics scenarios.

Table 6. Performance of highest ranked tour from ACO-PPD runs.

Quantity	Case Values							
	Base	**1**	**2**	**3**	**4**	**5**	**6**	**7**
Number of asteroid encounters	5	5	5	3	4	4	3	3
Summed merit of asteroids	4	4	4	5	2.5	2.5	5	4.5
Consumed Propellant, kg	125	115	95	40	75	65	40	65
Tour ΔV, km/s	15.7	15	14	7.5	10.1	10.5	7.5	8.5
Total Prox. Ops. Time, days	750	570	450	1750	1300	1200	1750	2150
Merit $\times$ Prox. Ops. Time, days	630	470	340	2670	660	610	2670	3530
Computation time*, sec	102	77	102	90	111	99	95	85

*For Matlab 2011a in Windows 7 Enterprise with 2.00 GHz dual processors.

CONCLUSIONS

The inclusion of a relative ranking of potential scientific return is shown to aid in the generation and selection of potential asteroid tours within the Sun-Jupiter L_4 Trojan swarm. The assignment of target importance can be based on unique features of interest, as is the case with the asteroids 624 Hektor and 3548 Eurybates, or upon physical properties common to sets of asteroids, e.g., the spectral type of the target bodies. Ant colony optimization, a heuristic search algorithm with many successful implementations to NP-hard problems outside mission analysis and design, is introduced and modified for astrodynamics applications. This stochastic algorithm, modeled after the foraging behavior of ant colonies wherein both exploration and pheromone following behaviors are exhibited, includes both local information based upon point-to-point transfer costs as well as global information based upon pheromone reinforcement of high quality tour sequences. While typically applied to relatively sparse, discrete networks, ant colony optimization methods are expanded to address trade spaces with dense sets of transfer options possessing continuous trade spaces; the parallel distribution of pheromone, in particular, is a powerful tool for exploiting the trade-off between transfer time and propellant cost inherent in all astrodynamics applications. Futhermore, ant colony optimization with parallel pheromone distribution can provide solutions not available to simplified search schemes but with a much reduced computational overhead compared to fully enumerated tree searches. Several avenues for future work remain open, particularly the application of ant colony optimization and relative target importance to other problems within astrodynamics.

ACKNOWLEDGEMENTS

This work was conducted at Purdue University and the Jet Propulsion Laboratory and is supported by a NASA Office of the Chief Technologist's Space Technology Research Fellowship, NASA Grant NNX12AM61H, and the Purdue Research Foundation. Many thanks to Wayne Schlei, who

helped immensely with the trajectory images and ACO discussions, the technical personnel at the Jet Propulsion Laboratory, Mission Design and Navigation Section. The authors also acknowledge the contributions of Prof. Seokcheon Lee of the Purdue University School of Industrial Engineering for introducing ACO to the authors as well as Andrew Rivkin of the John's Hopkins Applied Physics Laboratory for detailing interesting aspects of the Trojan asteroids.

REFERENCES

[1] N. Augustine, W. Austin, C. Chyba, C. Kennel, B. Bejmuk, E. Crawley, L. Lyles, L. Chiao, J. Greason, and S. Ride, "Seeking a Human Spaceflight Program Worthy of a Great Nation," tech. rep., U.S. Human Spaceflight Plans Committee, 2009.

[2] M. Brown, "Mission Concept Study: Trojan Tour Decadal Study," tech. rep., National Aeronautics and Space Administration, 2011. SDO-12348.

[3] J. R. Stuart and K. C. Howell, "An Automated Search Procedure to Generate Optimal Low-Thrust Rendezvous Tours of the Sun-Jupiter Trojan Asteroids," *23rd International Symposium on Space Flight Dynamics*, Pasadena, California, October 29 - November 2 2012. Paper No. ISSFD23-IMD1-2.

[4] J. R. Stuart, K. C. Howell, and R. S. Wilson, "Automated Design of Propellant-Optimal, End-to-End, Low-Thrust Trajectories for Trojan Asteroid Tours," *Journal of Spacecraft and Rockets*, In Press.

[5] J. R. Stuart, K. C. Howell, and R. S. Wilson, "Automated Design of Propellant-Optimal, End-to-End, Low-Thrust Trajectories for Trojan Asteroid Tours," *AAS/AIAA 23rd Space Flight Mechanics Meeting*, Kauai, Hawaii, February 10-14 2013, pp. 989–1005. Paper No. AAS-13-492.

[6] D. Goebel, J. Brophy, J. Polk, I. Katz, and J. Anderson, "Variable Specific Impulse High Power Ion Thruster," *Joint Propulsion Conference*, Tucson, Arizona, AIAA/ASME/SAE/ASEE, July 2005. Paper No. AIAA 2005-4246.

[7] T. W. Glover, F. R. C. Diaz, A. V. Ilin, and R. Vondra, "Projected Lunar Cargo Capabilities of High-Power VASIMR Propulsion," *Proceedings of 30th International Electric Propulsion Conference*, Florence, Italy, September 2007. IEPC-2007-244.

[8] K. Komurasaki, Y. Arakawa, and H. Takegahara, "An Overview of Electric and Advanced Propulsion Activities in Japan," *Proceedings of Third International Conference of Spacecraft Propulsion*, Cannes, France, October 2000, pp. 27–39.

[9] E. W. Dijkstra, "A note on two problems in connexion with graphs," *Numerische Mathematik*, Vol. 1, No. 1, 1959, pp. 269–271.

[10] A. H. . Land and A. G. Doig, "An Automatic Method of Solving Discrete Programming Problems," *Econometrica*, Vol. 28, No. 3, 1960, pp. 497–520.

[11] M. Dorigo, V. Maniezzo, and A. Colorni, "Positive Feedback as a Search Strategy," tech. rep., Dipartimento di Elettronica, Politecnico di Milano, Italy, 1991. Tech. Rep. 91-016.

[12] E. Bonabeau, M. Dorigo, and G. Theraulaz, *Swarm Intelligence: From Natural to Artificial Systems*. Oxford, England, United Kingdom: Oxford University Press, 1999.

[13] J. P. Emery, D. M. Burr, and D. Cruikshank, "Near-Infrared Spectroscopy of Trojan Asteroids: Evidence for Two Compositional Groups," 2013. *Astronomical Journal*, In Press.

[14] W. Calvin, "NASA's WISE Colors in Unknowns on Jupiter Asteroids," Jet Propulsion Laboratory Release, October 2012.

[15] S. J. Weidenschilling, "Hektor: Nature and Origin of a Binary Asteroid," *Icarus*, Vol. 44, No. 3, 1980, pp. 807–809.

[16] W. K. Hartmann and D. P. Cruikshank, "Hektor: The Largest Highly Elongated Asteroid," *Science*, Vol. 207, No. 4434, 1980, pp. 976–977.

[17] F. Marchis, F. Vachier, J. Durech, J. Berthier, M. Wong, P. Kalas, G. Duchene, and M. v. Dam, "Physical Characteristics of the Binary Trojan Asteroid (624) Hektor," *Asteroids, Comets, Meteors*, Niigata, Japan, May 16-20 2012.

[18] M. Broz and J. Rozehnal, "Eurybates - the only asteroid family among Trojans?," *Monthly Notices of the Royal Astronomical Society*, Vol. 414, No. 1, 2011, pp. 565–574.